Available online at www.sciencedirect.com

ScienceDirect

Energy Procedia 148 (2018) 511–518

Energy Procedia

www.elsevier.com/locate/procedia

73rd Conference of the Italian Thermal Machines Engineering Association (ATI 2018), 12-14 September 2018, Pisa, Italy

Numerical Study of a Wells Turbine with Variable Pitch Rotor Blades

Fabio Licheri[a,*], Antonello Climan[a], Pierpaolo Puddu[a], Francesco Cambuli[a], Tiziano Ghisu[a]

[a]*Department of Mechanical, Chemical and Materials Engineering, University of Cagliari, Italy*

Abstract

The Wells turbine is a self-rectifying axial turbine widely used in wave energy conversion systems based on the Oscillating Water Column (OWC) principle. In these systems, the periodic movement of the water surface inside a chamber open to the sea determines an alternating flow of air inside a duct, where a Wells turbine can be used to convert flow energy into mechanical energy. The architectural simplicity and the reliability of the Wells turbine represent its strengths, while the limited operating range due to the aerodynamic stall of the blades at high flow rates is probably its greatest drawback, as it limits the performance of the entire system. In this paper, a computational investigation on the aerodynamic performance of a variable-pitch Wells turbine is presented. Fluid dynamics simulations were conducted using commercial CFD software and focused on defining machine performance at different flow rates and blade pitch angles. Numerical results obtained have been exploited to define a pitching law, applicable for a period of operation of the OWC system, which allows to adapt the blade's setting angle to the variable relative flow, thus obtaining an extension of the machine's operating range, and maximizing energy production.

Keywords: Wave power conversion; Ocean energy; Wells turbine; Variable pitch rotor blades

1. Introduction

Among the various technologies proposed in the last decades to convert wave energy into electrical energy, the ones based on the principle of the Oscillating Water Column (OWC) are the most interesting to be used in plants located near- or on-shore [1]. The systems that use the OWC principle are composed of two different parts: an air chamber that converts the wave motion into pneumatic energy in the form of a bi-directional air flow, and a power take-off capable to use this air flow to produce mechanical energy available on a shaft.
Between the different air turbines proposed [2], the Wells turbine invented by Dr. A. A. Wells in 1979 [3] is one of the most attractive. Due to the symmetrical profile of its blades, the Wells turbine is a self-rectifying turbine constructively simple and reliable. Many authors have studied this turbine, both numerically [4, 5] and experimentally [6, 7, 8, 9],

*Corresponding author. E-mail: fabiolicheri@outlook.it

10.1016/j.egypro.2018.08.127

Nomenclature

β	flow angle	P^*	non-dimensional static pressure drop
η	aerodynamic efficiency $(X/(Y\phi))$	R	aerodynamic resultant
γ	blade setting angle	r_m	mean radius $((r_t + r_h)/2))$
μ	fluid viscosity	r_h	hub radius
ω	angular velocity	r_t	tip radius
ϕ	flow coefficient	T	torque
ρ	density	T^*	non-dimensional torque
τ_w	wall shear stress	U	blade speed (ωr)
c	blade chord	V	absolute axial velocity
D	drag force	W	relative velocity
i	effective flow incidence $(\beta - \gamma)$	X	component of R along x direction
L	lift force	Y	component of R along y direction
n	rotational speed	y^+	non-dimensional wall distance $(y\sqrt{\rho\tau_w}/\mu)$
P	static pressure	z	blade number

in order to determine its behavior and its advantages and disadvantages. Its most important drawbacks are the poor starting characteristic, a relative low efficiency and a limited range of operation due to stall.

In order to delay the occurrence of stall at high flow rates, some authors [10, 11] have studied a novel model of Wells turbine with a row of guide vanes on both sides of the rotor. They showed that this solution can increase the turbine operating range while improving its efficiency. Other authors [12] proposed the use of forward swept blades for Wells turbine and they determined numerically the optimal configuration to maximize the power output of the turbine. Another possible solution to delay the stall onset consists in a Wells turbine with variable pitch rotor blades [13, 14, 15, 16]. This solution, employed for example in the Azores OWC Pilot Plant [17, 18], consists in a non-conventional rotor where the blades can modify their pitch angle. The one with a passive pitch control [16] is geometrically simpler and less expensive to manufacture in comparison with one using active pitch controlled blades [17]. In the former solution the aerodynamic moment is used to rotate the blades. On the other hand, with an active pitch control it is possible to release the movement of the blades from the aerodynamic force and thus it is possible to establish different pitch laws to maximize the energy production for every flow condition.

This work reports a 2D numerical investigation on a Wells turbine with variable pitch. The work is focused on maximizing the energy production of the turbine by varying blade pitch angle as a function of the incident flow conditions. A comparison between the performance obtained with an active and a passive control on the blade rotation has been reported. The geometry of the problem analyzed is the same of the OWC experimental setup located in the laboratory of the D.I.M.C.M. at the University of Cagliari.

2. Methodology

The geometry studied in this work is the same of the high solidity Wells turbine with fixed blades employed in the OWC experimental rig located in the D.I.M.C.M. laboratory. Its main parameters are reported in Table 1.

Table 1. Wells turbine data and parameters

Airfoil	NACA0015	Blade Number	14
Rotor Tip Diameter	250 mm	Solidity at Tip Radius	0.642
Rotor Hub Diameter	190 mm	Chord Length	36 mm
Rotational Speed	3000 rpm	Wave Period	9 s

Figure 1 reports the convention used for the sign of pitch angle with respect to the two directions of the flow in an OWC system, together with velocity triangles and aerodynamic forces.

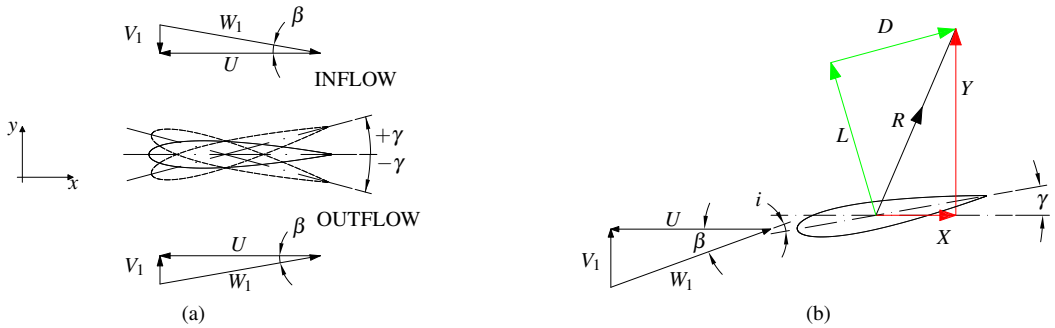

Fig. 1. Convention for the blade angle with respect flow directions (a) and aerodynamic forces acting on a blade (b)

A single blade vane in two dimensions has been simulated. The numerical grid (Figure 2) was generated using the commercial software Ansys IcemCFD®. A multi-block structure has been used: the region surrounding the blade profile has been discretized with a structured C-grid that was set to rotate together with the profile to capture the boundary layer flow correctly; a central zone around the C-grid is discretized using unstructured triangular cells to allow mesh deformation and re-meshing, in case the cell quality had gone below a given value, during blade rotation (minumum and maximum size equal to the initial values in the region, and a minimum skewness of 0.7). The zones adjacent to inlet and outlet sections are structured. A refinement study was conducted to ensure grid independent results. About 90000 cells were used, with a y^+ of the order of 1. Periodic conditions at the boundary edges (left and right) of the grid were used to describe blade interaction effects.

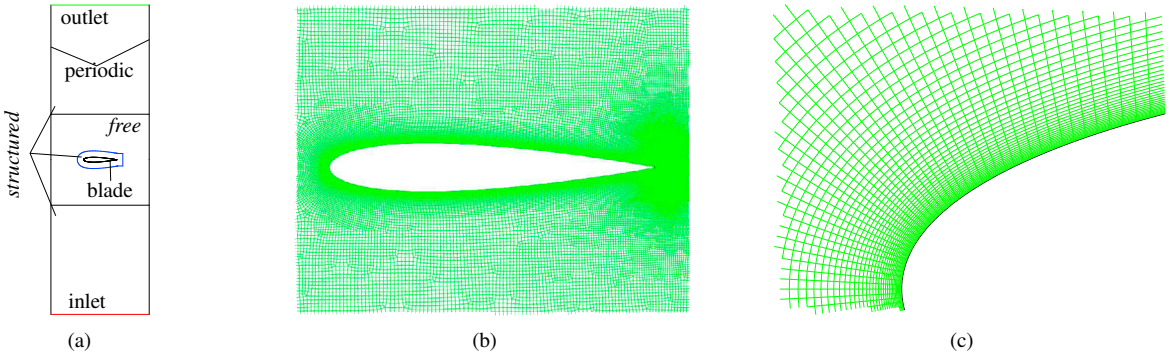

Fig. 2. Blocking scheme (a) and computational mesh for null blade angle (b) and close-up view of the leading edge region (c)

Numerical simulations have been conducted using the commercial CFD software Ansys Fluent® 17.0. The $k-\omega$ SST model has been selected for the turbulence closure while the SIMPLEC algorithm has been used for pressure-velocity coupling, a second-order upwind scheme for discretizing convective terms and a second-order centered scheme for pressure and viscous terms. The absolute velocity at the inlet section was set by means of a UDF (*User Defined Function*).

In order to determine when the stall occurs for each blade setting angle γ, two types of simulations were conducted. The first ones, called *quasi-static simulations* (Q-SS), were conducted by running unsteady RANS simulations with fixed boundary conditions , initializing the flow field with the solution for the previous angle of attack. This approach allowed better convergence with respect to steady simulations, especially at conditions near stall. The second ones, called *dynamic simulations* (DS), were conducted by varying the inlet axial velocity continuously from zero (flow rate equal to zero) until the stall onset. In DS, the rate of change of flow angle was set to the same value experienced by the turbine during actual operation, but the simulation was stopped after a degradation in performance suggested the occurrence of stall.

Dynamic simulations were carried out also to simulate the behavior of a conventional Wells turbine, an active pitch

controlled blade and a passive pitch controlled blade under a typical OWC air flow. The pitch angle, both for active and passive controlled turbine, was set by using another UDF. For the active controlled blade, the UDF provides the rate of change of the pitch angle as a function of the flow coefficient and is based on the pitch law obtained from Q-SS and DS. For the passive controlled blade, the UDF solves the differential equation otained balancing the forces acting on the blade (inertial, viscous and aerodynamic forces, and an opposite force representing the action of a spring).
All dynamic simulations were run for three working periods and no difference between the results of second and third period was observed. The time-step for dynamic simulations was chosen equal to 5×10^{-5} s after an investigation on its minimum value necessary to ensure the absence of any phase error due to insufficient temporal discretization.

3. Results

3.1. Correlation between blade setting angle and flow parameters

Figure 3 (left) shows the torque coefficient T^* vs the flow coefficient ϕ for several blade setting angles. Points refer to the results obtained from Q-SS simulations while lines report the results obtained from DS. These parameters were calculated using equations (1).

$$T^* = \frac{-X\,z}{\rho\,\omega^2\,r_m^4}; \qquad \phi = \frac{V_a}{\omega\,r_m}; \qquad P^* = \frac{\Delta P}{\rho\,\omega^2\,r_m^2}; \qquad \eta = \frac{X}{Y}\frac{1}{\phi} \tag{1}$$

Figure 3 (left) allows to observe the stall onset, highlighted with a rapid collapse of the torque coefficient. For the non-rotated blade the stall occurs for a flow coefficient of 0.19 while the maximum flow coefficient before stall is around 0.5 for the 10°-pitch blade. Figure 3 (left) shows the good agreement between the results obtained with static and dynamic simulations. This is a consequence of the negligible contribution of dynamic effects in Wells turbines [19, 20, 21, 22], determined by its low operating non-dimensional frequency. By extrapolating the maximum values of T^* for each blade position, a pitch angle variation law for the blade was defined, Figure 3 (right), that consists in a linear correlation between blade pitch angle and flow coefficient.

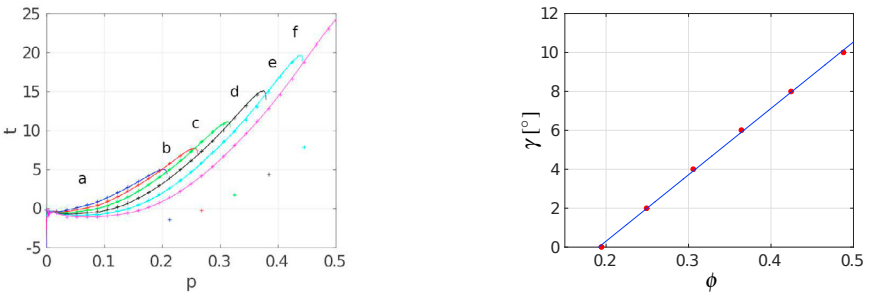

Fig. 3. Torque coefficient for several blade setting angles evaluated from Q-SS (points) and DS (lines), (left), and pitch law to maximize the torque coefficient obtained from Q-SS, (right)

3.2. Comparison between fixed turbine and variable-pitch turbine

In order to understand the behavior of a Wells turbine with variable pitch rotor blades when it works under dynamic conditions typical of an OWC device, the pitch law was tested in a simulation where the absolute velocity at the turbine inlet, so the flow coefficient, was varied sinusoidally. The correlation previously shown, was applied in combination with a UDF for the inlet velocity determining a maximum flow coefficient equal to 0.5, symmetrically during inflow

and outflow phases. The law applied is shown in Figure 4 and it consists in a linear variation of the blade angle for values of the flow coefficient larger that the one determining stall for the zero-pitch blade. The result obtained by using this law in terms of torque coefficient versus flow coefficient and non-dimensional pressure drop coefficient versus flow coefficient, Figure 4, were compared with the corresponding results estimated for a conventional Wells turbine with fixed blades operating under a maximum flow coefficient equal to 0.19, which represents its operating limit.

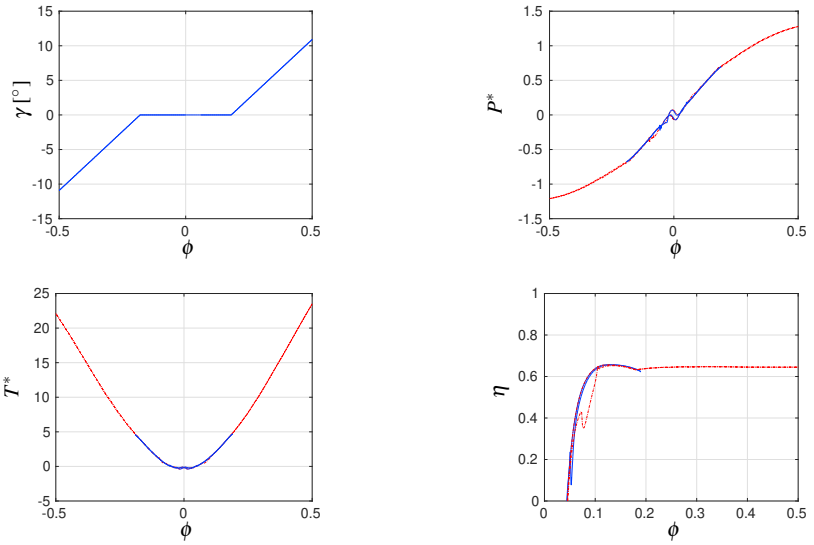

Fig. 4. Angle variation law (top-left) and comparison of torque coefficient (bottom-left), non-dimensional pressure drop coefficient (top-right) and aerodynamic efficiency (bottom-right) obtained with variable pitch blades (red dash-dot line) and fixed blades (blue continuous line)

The comparison shows how the variable pitch rotor turbine is capable to extend the operating range of the conventional Wells turbine that is limited to operate with a maximum flow coefficient of about ± 0.19. Due to the highest intensity of the flow, the torque acting on the turbine, proportional to the energy production, can be increased. The same conclusion can be drawn for the non-dimensional pressure coefficient. The variable pitch law allow the aerodynamic efficiency approximately constant at the value achieved by the fixed turbine just before stall. By observing the performance coefficients (Figure 4), it is evident how both fixed and variable-pitch blade turbine do not show any visible in performance between acceleration and deceleration phases (hysteresis). This result is in agreement with the results that showed how the aerodynamic hysteresis in Wells turbine is negligilbe [20], given the low non-dimensional frequency the turbine operates at.

3.3. Comparison between active pitch controlled turbine and self pitch controlled turbine

Another numerical test was carried out to simulate the behavior of a Wells turbine with self pitch controlled blades. In this case the blade rotation is a function of the difference between aerodynamic moment and the opposing moment produced by a spring. As described in [13], an airfoil set at a certain angle of incidence generates a pitching moment about a pivot that can be used to rotate the blade. To make sure that the rotation is in the direction required to decrease its incidence it is necessary to locate the pivot in a position between the leading edge and the pressure center of the blade, or of the airfoil in general, where the resultant $\vec{R}$ of the aerodynamic force acts. For a NACA0015 profile the position of pressure center is not constant with the blade angle, but is located around the $25 \div 30\%$ of the blade chord. A pivot position at 12.5% of the blade chord has therefore been chosen. The UDF that controlled the blade rotation has been modified in order to solve the differential balance equation (2) between the pitch moment and the blade rotation. The equation has been solved numerically with a semi-implicit time marching method:

$$I_p\ddot{\gamma} + \beta_m\dot{\gamma} + k_m\gamma = C_M \qquad (2)$$

$$\begin{cases} \dot{\gamma}_{j+1} = \dot{\gamma}_j - \dfrac{\beta_m}{I_p}\dot{\gamma}_j\Delta t + \dfrac{C_M - k_m\gamma_j}{I_p}\Delta t \\ \gamma_{j+1} = \gamma j + \dot{\gamma}_j\Delta t \end{cases} \qquad (3)$$

which were then solved in an UDF that was linked to the CFD solver. I_p is the polar moment of inertia of the blade section (2.93×10^{-5} kg m^2/m), β_m is the damping coefficient (0.05 N m s/m), k_m is the elastic constant (3.16 N m/m), C_M is the pitching moment acting on the section, j is the temporal step and Δt the time-step size. Parameter values in (3) were set to obtain the desired variation in pitch angle at $\phi = 0.5$. I_p was evaluated as the product between the polar moment of the blade section and the density of the aluminum (3000 kg/m^3). The damping coefficient β_m was set to obtain a system response with no oscillations. Elastic spring coefficient k_m was set by fixing the acceleration $\ddot{\gamma}$ and the velocity $\dot{\gamma}$ equal to zero for the maximum flow coefficient; with these two initial conditions, equation (3) was reduced to $k_m\gamma = C_M(\phi = \phi^M)$, with k_m the only unknown parameter.

Figure 5 reports a comparison between passive and active pitch controlled blades in terms of their performance, torque coefficient non-dimensional pressure drop and aerodynamic efficiency, and in terms of their pitch laws. The torque coefficient for passive turbine is always lower than the one for the active turbine because with a passive system the blades rotate according to their system parameters (k_m, β_m and I_p) that have been set to perform a specific operating range. On the other hand, the pressure drop is marginally lower for the self controlled turbine. The maximum aerodynamic efficiency, on the contrary, is higher for the self controlled one respect to the active controlled one, but it is not constant with the flow coefficient. The possibility to set a pitch law to maximize the aerodynamic efficiency, highlighted by this last plot, were not evaluated in this work.

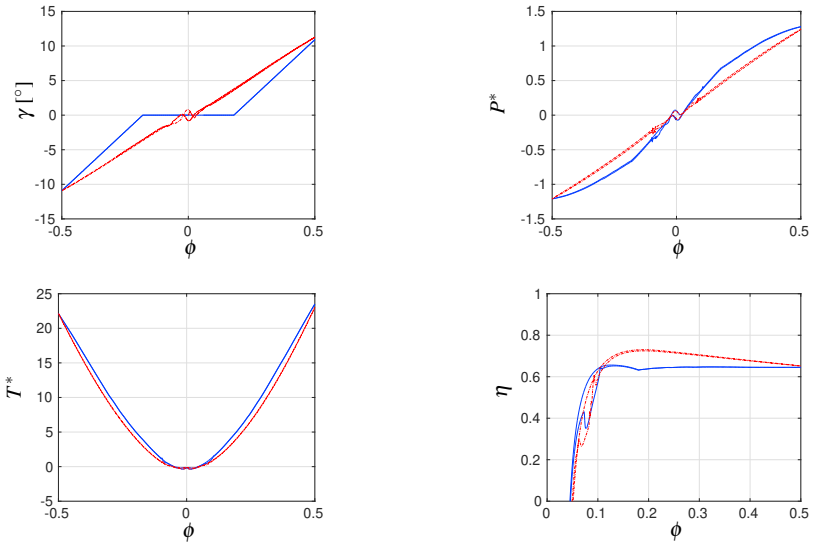

Fig. 5. Angle variation law (top-left), comparison of torque coefficient (bottom-left), non-dimensional pressure drop coefficient (top-right) and aerodynamic efficiency (bottom-right) obtained with active (blu continuous line) and passive variable pitch blades (red dash-dot line)

Also by observing the results obtained for the passive pitch controlled blade turbine under a typical flow for an OWC, it is impossible to appreciate a real effect of hysteresis between acceleration and deceleration phases. Similar conclusions can be drawn by observing Figure 6, where the contour plots of non-dimensional relative velocity around the blade for symmetrical position around a quarter period are compared for active and passive pitch controlled turbine. This is again in agreement with the results of [19, 20, 21, 22], who showed how dynamic effects in Wells turbine are negligible, as an effect of the low value of the non-dimensional frequency they operate at.

Figure 7 shows a comparison of the pressure coefficient during the accelerating phase for active and passive pitch-

controlled turbine. A noticeable difference only exists for low values of the flow coefficient, where the active turbine has not yet rotated about its pivot in the active control case.

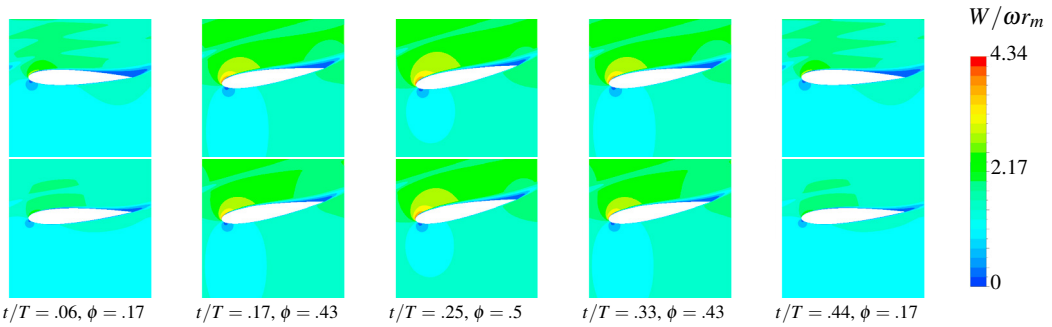

Fig. 6. Comparison between active (top) and passive (bottom) pitch controlled blades turbine respect to non-dimensional relative velocity contours around the blade at symmetrical position around maximum flow coefficient ($\phi = 0.5$)

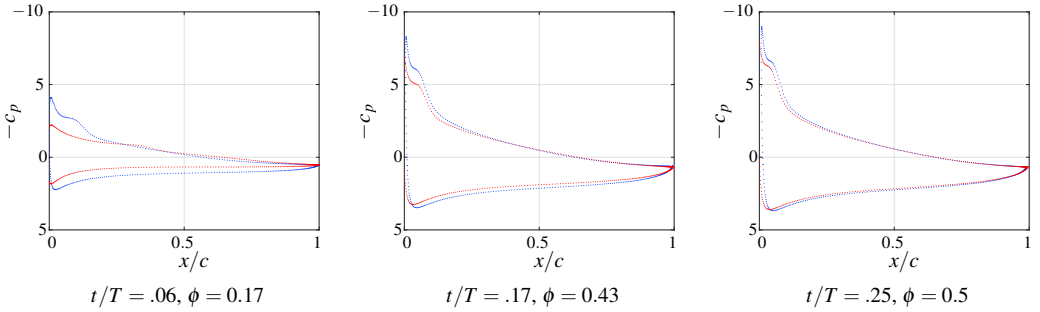

Fig. 7. Pressure coefficient comparison between active (blue) and passive (red) pitch controlled blades turbine for different values of flow coefficient in accelerating phase

Figure 6 highlights the absence of hysteresis during accelerating and decelerating phases by comparing the velocity field around the blade for the same flow coefficient reached during these two phases. It also shows the different angle reached by the blades controlled with active or passive system when the flow coefficient is different from its maximum value, especially when it is equal to 0.17. In Figure 7 is possible to appreciate, better than in Figure 6, how for the same flow coefficient the active pitch controlled blades are nearest the stall limit than the passive ones. This confirm the predictions about the torque coefficient, that can be maximized by using an active pitch law calibrated for a certain period of the wave.

4. Conclusions

In this work, the performance of a Wells turbine with active and passive pitch-controlled blades was studied using numerical simulations. A pitch law was determined, by comparing *quasi-static* and *dynamic* simulations run for several fixed blade pitch angles, in order to maximize the energy production of the turbine. The law was applied under a sinusoidal air flow to simulate the flow conditions in an OWC plant. The results obtained for a Wells turbine with active and passive pitch controlled blades were compared with similar results obtained for a conventional turbine, demonstrating a significant increase in turbine working range.

The comparison between the two control methods showed that the performance obtained with an active pitch law are better, in terms of output torque, than the performance reached by a turbine with self pitch controlled blades designed to operate in the same working range, while the self pitch controlled turbine can reach higher aerodynamic efficiency than the active pitch controlled turbine.

In all simulations, dynamic effects have always found to be negligible, meaning that the pitching law can be defined without any loss in accuracy using static performance data.
In conclusion, while an active controller can maximize the energy production for a variable pitch Wells turbine under different air flows, a passive controller designed for the same turbine is less expensive and simpler to design than the active one and achieves performance only marginally lower than the former, therefore representing an ideal choice to increase the turbine's operating range.

References

[1] A. F. O. Falcao, Wave energy utilization: A review of the technologies, Renewable and Sustainable Energy Reviews 14 (3) (2010) 899–918. doi:10.1016/j.rser.2009.11.003.
[2] A. Falcao, L. Gato, Air turbines, Comprehensive Renewable Energy 8 (2012) 111–149. doi:10.1016/B978-0-08-087872-0.00805-2.
[3] A. Wells, Fluid Driven Rotary Transducer - BR. Pat. 1595700 (1976).
[4] M. Torresi, S. M. Camporeale, P. D. Strippoli, G. Pascazio, Accurate numerical simulation of a high solidity Wells turbine, Renewable Energy 33 (4) (2008) 735–747. doi:10.1016/j.renene.2007.04.006.
[5] T. M. Premkumar, M. Ashish, T. Banu Prakash, D. Thulasiram, Numerical analysis of Wells turbine, Applied Mechanics and Materials 592-594 (2014) 1125–1129. doi:10.4028/www.scientific.net/AMM.592-594.1125.
[6] S. Raghunathan, O. O. Ombaka, Effect of frequency of air flow on the performance of the Wells turbine, International Journal of Heat and Fluid Flow 6 (2) (1985) 127–132. doi:10.1016/0142-727X(85)90049-9.
[7] M. Webster, L. M. C. Gato, P. R. S. White, Variation of blade shape and its effect on the performance of the Wells turbine, International Journal of Ambient Energy 19 (3) (1998) 149–156. doi:10.1080/01430750.1998.9675702.
[8] L. M. C. Gato, M. Webster, An experimental investigation into the effect of rotor blade sweep on the performance of the variable-pitch Wells turbine, Proceedings of the Institution of Mechanical Engineers, Part A: Journal of Power and Energy 215 (5) (2001) 611–622. doi:10.1243/0957650011538848.
[9] P. Puddu, M. Paderi, C. Manca, Aerodynamic characterization of a Wells turbine under bi-directional airflow, Energy Procedia 45 (2014) 278–287. doi:10.1016/j.egypro.2014.01.030.
[10] L. Gato, A. Falcao, Performance of the wells turbine with a double row of guide vanes, JSME INT. J. SERIES II 33 (1990) 265–271. doi:https://doi.org/10.1299/jsmeb1988.33.2_265.
[11] M. Takao, T. Setoguchi, T. H. Kim, K. Kaneko, M. Inoue, The performance of a wells turbine with 3d guide vanes, International Journal of Offshore and Polar Engineering 11 (2001) 05.
[12] P. Halder, S. H. Rhee, A. Samad, Numerical optimization of Wells turbine for wave energy extraction, International Journal of Naval Architecture and Ocean Engineering 9 (1) (2017) 11–24. doi:10.1016/j.ijnaoe.2016.06.008.
[13] M. Inoue, K. Kaneko, T. Setoguchi, H. Hamakawa, Air turbine with self-pitch controlled blades for wave power generator (Estimation of performance by model testing), JSME International Journal,Series II 32 (1) (1989) 19–24.
[14] L. Gato, A. de O. Falcao, Aerodynamics of the wells turbine: control by swinging rotor-blades, International Journal of Mechanical Sciences 31 (6) (1989) 425 – 434. doi:https://doi.org/10.1016/0020-7403(89)90078-7.
[15] L. M. C. Gato, L. R. C. Eca, a. F. D. O. Falcao, Performance of the Wells Turbine With Variable Pitch Rotor Blades, Journal of Energy Resources Technology 113 (3) (1991) 141–146. doi:10.1115/1.2905794.
[16] T. H. Kim, T. Setoguchi, M. Takao, K. Kaneko, S. Santhakumar, Study of turbine with self-pitch-controlled blades for wave energy conversion, International Journal of Thermal Sciences 41 (1) (2002) 101–107. doi:10.1016/S1290-0729(01)01308-4.
[17] J. R. M. Taylor, N. J. Caldwell, Design and construction of the variable-pitch air turbine for the Azores wave energy plant, In: Proceedings of the 3rd European Wave Power Conference (October) (1998) 7–12.
[18] W. K. Tease, Dynamic response of a variable pitch Wells turbine, Acta Anaesthesiologica Scandinavica 53 (6) (2009) 1341–7. doi:10.1111/j.1399-6576.2009.02081.x.
[19] T. Ghisu, P. Puddu, F. Cambuli, Numerical analysis of a wells turbine at different non-dimensional piston frequencies, Journal of Thermal Science 24 (6) (2015) 535–543. doi:10.1007/s11630-015-0819-6.
[20] T. Ghisu, P. Puddu, F. Cambuli, Physical explanation of the hysteresis in wells turbines: a critical reconsideration, Journal of Fluids Engineering, Transaction of the ASME 138 (11) (2016) 1–9. doi:10.1115/1.4033320.
[21] T. Ghisu, P. Puddu, F. Cambuli, A detailed analysis of the unsteady flow within a Wells turbine 231 (3) (2017) 197–214. doi:10.1177/0957650917691640.
[22] T. Ghisu, P. Puddu, F. Cambuli, N. Mandas, P. Seshadri, Parks, Discussion on "Performance analysis of Wells turbine blades using the entropy generation minimization method" by Shehata, A. S., Saqr, K. M., Xiao, Q., Shahadeh, M. F. and Day, A., Renewable Energy 118. doi:10.1016/j.renene.2017.10.107.